A numerical survey of artificial atoms –Quantum Dots in two dimensions

Diploma Work

Erik Waltersson
Stockholm University, Department of Physics

29th October 2003

Stockholm University
Department of Physics
http://www.physto.se/

Erik Waltersson:
walter@physto.se

Supervisor:

Prof. Eva Lindroth

Sammanfattning på svenska

Egenskaper hos *tvådimensionella cirkulära kvantprickar* undersöks ur en teoretisk och beräkningsteknisk synvinkel. Vågfunktioner uttryckes i *B-splines* och den tidsoberoende Schrödingerekvationen löses genom *exakt diagonalisering*.

Beräkningarna genomföres genom användadet av de två metoderna *local density* och *spin-polarized Hartree-Fock* för beskrivningen av utbytesväxelverkan mellan elektroner. De två metoderna jämföres och för- och nackdelar mellan metoderna diskuteras.

Skalstrukturen hos *tvådimensionella cirkulära kvantprickar* visas genom additionsspektra i de båda teorierna. Spektrumen jämföres med experimentella resultat. *Hund's första regel* uppkommer som en konsekvens av elektronkonfigurationen i *Hartree-Fock* beräkningarna.

Därutöver undersöks hur egenskaperna ändras när ett externt magnetfält appliceras. Resultaten stämmer häpnadsväckande bra för *local density* metoden när de jämföres med experimentella data. Emellertid lyckas *Hartree-Fock* beräkningarna påvisa vissa magnetiska egenskaper som *local density* beräkningarna ej kan visa.

Abstract

Properties of *two dimensional circular quantum dots* are investigated from a theoretical and computational point of view. Wavefunctions are expanded in *B-splines* and the time independent Schrödinger equation is solved by an *exact diagonalization method*.

The calculations are performed using both *local density* and *spin-polarized Hartree-Fock* methods for the exchange interaction between electrons. The two methods are compared and their advantages and disadvantages are discussed.

The shell structure of *two dimensional circular quantum dots* are shown by the addition energy spectra in both theories. The spectra are compared with experimental result. *Hund's first rule* appear as a consequence of the electron configuration in the *Hartree-Fock* calculations.

Moreover it is explored how the properties change when an external magnetic field is applied. The results agree surprisingly well for the *local density* calculations when compared with experimental results. The *Hartree-Fock* calculations however, succeed to show some magnetic properties that the *local density* calculations fail to.

Contents

Chapter 1

Introduction

During the last 20 years a new research area in condensed-matter physics has been explored. More advanced experimental techniques allow for the possibility of artificial creation of low-dimensional quantum confinements containing just a few electrons. Nowadays the techniques are so advanced that one can start with a single electron in the confinement and then add electrons, one by one[1]. Such small man made fermion systems are usually called quantum dots. Quantum dot properties resembles atomic and nuclear properties in several ways, for example the shell structure.

There are a couple of ways to construct quantum dots, but since this is a theoretical work not limited to a specific experimental technique, no specific experimental technique will be explained in detail[1]. However all experimental techniques trap electrons from the conduction band of the semi-conductor in some sort of man made potential[1][2][3][4]. One way of trapping the electrons is described briefly in figure 1.1.

The properties of the quantum dots can be controlled and changed by for example applying a magnetic field, changing semi-conductor material or by changing the gate voltage.

In this work some physical properties of two dimensional circular quantum dots will be described from a theoretical and computational approach and in some cases the result will be compared to other studies, theoretical as well as experimental.

[1]Another reason is that the knowledge of the experimental techniques yours truly posses is limited.

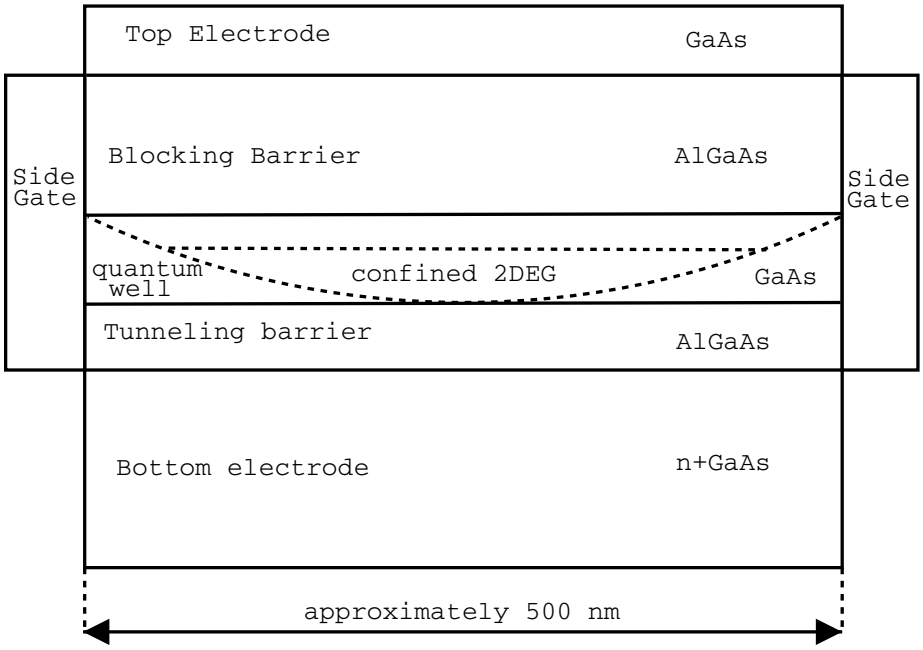

Figure 1.1: *Schematic illustration of an experimental technique. The difference in Fermi energies between the different semi-conductor materials (AlGaAs, GaAs, AlGaAs) forms a quantum well where a two-dimensional electron gas (2DEG) is trapped. A voltage is applied over the side gates. This voltage form the confining potential. In order to add an electron a voltage is applied over the top and bottom electrodes. When the voltage is strong enough a charge carrier from the n-doped semi-conductor tunnels into the dot.*

Chapter 2

Theory

2.1 The Mean-field approach and self-consistency

The mean-field approximation suggests that each electron moves independently of the other electrons in a circular-symmetric[1] field produced by the surrounding and the other electrons. When the Schrödinger equation is solved, one calculates how the occupied states effects the surrounding[2] and then calculate the new electron states. This procedure is repeated until the energy values of all occupied orbitals are consistent[3] between iterations. When this is achieved one has reached self-consistency.

2.2 Effective atomic units

The electrons in a quantum dot belong to the conduction band of the semiconductor. As customary, effects due to their interaction with the lattice and the valence and core electrons can be accounted for in the so called *effective-mass approximation*[18][19]. In this approximation the electrons in the quantum dot form a separate interacting electron system, each electron with the effective mass m^*, and their Coulomb interaction with each other is scaled with the relative dielectric constant, ϵ_r, of the semi-conductor.

For example GaAs has $m^* \approx 0.067m_e$ and $\epsilon_r \approx 13.5$. This implies for example that the kinetic energy, $\mathbf{p}^2/(2m^*)$, gets larger and the electron-electron interaction, $e^2/(4\pi\epsilon_0\epsilon_r|\mathbf{r}_1 - \mathbf{r}_2|)$, gets weaker than they would have been in a free electron gas.

In atomic-physics so called atomic units are frequently adopted to make things easy[6]. Here however one must modify this a bit and use so called *effective atomic units*. When using this convention one measures quantities in units of some suitable atomic constants. For example one measures the mass in units of m^* and charge in units of e. This has the effect that in effective atomic units

$$e = m* = \hbar = 4\pi\epsilon\epsilon_r = a_B^* = 1. \tag{2.1}$$

[1] In atomic physics this is spherical-symmetric due to that atoms are three dimensional.
[2] i.e. How they change the potential.
[3] In reality one must set a numerical value to what consistency is.

Note that the units change when changing the semi-conductor material because ϵ_r and m^* then changes. *Effective atomic units* will be used from now on when nothing else is mentioned.

2.3 The Schrödinger equation

The time independent Scrödinger equation is written

$$\hat{H}|\Psi_n(\mathbf{r})\rangle = E_n|\Psi_n(\mathbf{r})\rangle, \tag{2.2}$$

where the Hamilton operator is

$$\hat{H} = \left(\frac{\hat{\mathbf{p}}^2}{2} + V(\mathbf{r})\right). \tag{2.3}$$

If we assume that the potential is circular symmetric then the solution of (2.2) is separable. That is the solution can be written

$$|\Psi_{nm}(\mathbf{r})\rangle = |u_{nm}(r)\rangle|e^{im\theta}\rangle, \tag{2.4}$$

where $\mathbf{r} = x\hat{\mathbf{x}} + y\hat{\mathbf{y}}$ is the position vector in the plane, r the radius in polar coordinates, θ the polar angle, n the radial quantum number and m the angular quantum number.

To solve the Schrödinger equation we expand the radial part of the wavefunctions in so called B-splines[4] labeled B_i with coefficients c_i in the following way

$$|u_{nm}(r)\rangle = \sum_i c_{inm}|B_i\rangle, \tag{2.5}$$

so that the total wavefunction

$$|\Psi_{nm}(\mathbf{r})\rangle = \sum_i c_{inm}|B_i\rangle|e^{im\theta}\rangle. \tag{2.6}$$

Multiplication of (2.2) with $\langle B_j e^{im\theta}|$ from the left when using the expansion (2.6) yields

$$\sum_i c_{inm}\underbrace{\langle B_j e^{im\theta}|\hat{H}|B_i e^{im\theta}\rangle}_{\mathbf{B}_{ji}} = \sum_i E_n c_{inm}\underbrace{\langle B_j|B_i\rangle}_{\mathbf{U}_{ji}}. \tag{2.7}$$

Note that in general $U_{ji} \neq \delta_{ji}$ due to that the B-splines are not in general orthogonal if they are of order greater than one. Hence the Schrödinger equation can be written in matrix form

$$\mathbf{U}^{-1}\mathbf{B}\mathbf{c}_n = E_n\mathbf{c}_n. \tag{2.8}$$

Solving the Schrödinger equation now transforms into solving a standard eigenvalue problem. This implies that the eigenvalues and the eigenstates of $\mathbf{U}^{-1}\mathbf{B}$ can be found by standard numerical techniques. In equation (2.8) E_n already are the eigenvalues of the Hamilton-operator. Obtaining the eigenstates of the Hamilton-operator is simply a task of sorting the eigenfunctions of (2.8) by the size of E_n and then using equation (2.6).

[4]See appendix A

2.4 The Matrix element

Since we are working with a 2D quantum dot, the motion is constrained to the xy-plane. Then we know that the kinetic energy operator of equation (2.2) can be written as

$$\hat{T} = \frac{1}{2}\hat{\mathbf{p}}^2 = \frac{1}{2}\left(\hat{p}_x^2 + \hat{p}_y^2\right). \tag{2.9}$$

Furthermore we know that

$$\hat{p}_k = -i\hbar\frac{\partial}{\partial k} \Rightarrow \hat{p}_k^2 = \left(-i\hbar\frac{\partial}{\partial k}\right)^* \left(-i\hbar\frac{\partial}{\partial k}\right) = \hbar^2\left(\frac{\partial}{\partial k}\right)^* \left(\frac{\partial}{\partial k}\right); k = x, y \tag{2.10}$$

and that in polar coordinates (r, θ)

$$\begin{cases} \frac{\partial}{\partial x} = & \cos\theta\frac{\partial}{\partial r} - \frac{\sin\theta}{r}\frac{\partial}{\partial\theta} \\ \frac{\partial}{\partial y} = & \sin\theta\frac{\partial}{\partial r} + \frac{\cos\theta}{r}\frac{\partial}{\partial\theta}. \end{cases} \tag{2.11}$$

Equations (2.9),(2.10) and (2.11) implies for some functions $f_j(r)e^{im\theta}$ and $f_i(r)e^{im\theta}$ that

$$\begin{aligned} &\langle f_j e^{im\theta}|\hat{\mathbf{p}}^2|f_i e^{im\theta}\rangle = \\ &\hbar^2\int_0^\infty dr\int_0^{2\pi} d\theta\Big(\left[\left(\cos\theta\tfrac{\partial}{\partial r} - \tfrac{\sin\theta}{r}\tfrac{\partial}{\partial\theta}\right) f_j e^{im\theta}\right]^* \left[\left(\cos\theta\tfrac{\partial}{\partial r} - \tfrac{\sin\theta}{r}\tfrac{\partial}{\partial\theta}\right) f_i e^{im\theta}\right] + \\ &\left[\left(\sin\theta\tfrac{\partial}{\partial r} + \tfrac{\cos\theta}{r}\tfrac{\partial}{\partial\theta}\right) f_j e^{im\theta}\right]^* \left[\left(\sin\theta\tfrac{\partial}{\partial r} + \tfrac{\cos\theta}{r}\tfrac{\partial}{\partial\theta}\right) f_i e^{im\theta}\right]\Big) \\ &= \hbar^2\int_0^\infty dr\int_0^{2\pi} d\theta\left[\tfrac{\partial f_j}{\partial r}\tfrac{\partial f_j}{\partial r} + \tfrac{m^2}{r^2} f_j f_i\right]. \end{aligned} \tag{2.12}$$

We know by equation (2.6) that the wavefunction can be expressed as $f_i e^{im\theta}$. Hence the matrix element becomes

$$\langle B_j e^{im\theta}|\hat{H}|B_i e^{im\theta}\rangle = \int_0^\infty dr\int_0^{2\pi} d\theta\left[\frac{1}{2}\frac{\partial B_j}{\partial r}\frac{\partial B_i}{\partial r} + \frac{1}{2}B_j\frac{m^2}{r^2}B_i + B_j V(r) B_i\right]. \tag{2.13}$$

2.5 The Potential

2.5.1 The Surrounding

Initially it is assumed that the surroundings contribute to the potential as a 2D harmonic potential

$$V_\omega = \frac{1}{2}\omega^2 r^2, \tag{2.14}$$

where r is the radius in the xy-plane and ω is the effective confinement strength.

Most theoretical work done on quantum dots is based on this assumption and this due to an article of Kumar, Laux and Stern[5]. They show through a self consistent Hartree approach that despite a square geometry of the gate the results agree with those found for a parabolic confinement. Note that the experiments themselves tell nothing about what values of ω are reasonable. This then becomes a parameter that can be chosen so that the calculations agree with experimental results.

2.5.2 The interaction between electrons

The Pauli exclusion principle

The Pauli exclusion principle states that two electrons, in general two fermions, or more can't be in the same state at the same time. This together with the fact that electrons are indistinguishable implies that the *N-particle wavefunction*, $\Phi_{12..N}(\mathbf{x}_1, \mathbf{x}_2, ..., \mathbf{x}_N)$, must be antisymmetric under particle exchange. That is

$$\Phi_{12..N}(\mathbf{x}_1, \mathbf{x}_2, ..., \mathbf{x}_i, ..., \mathbf{x}_j, ..., \mathbf{x}_N) = -\Phi_{12..N}(\mathbf{x}_1, \mathbf{x}_2, ..., \mathbf{x}_j, ..., \mathbf{x}_i, ..., \mathbf{x}_N) \tag{2.15}$$

where $\mathbf{x}_k$ is the position vector and the numbers $1, 2, \ldots, N$ correspond to the set of quantum numbers particle $1, 2, \ldots, N$ have respectively. A handy way to construct a normalized N-particle wavefunction from single particle wavefunctions is by a so called *Slater-determinant*:

$$\Phi_{12..N}(\mathbf{x}_1, \mathbf{x}_2, ..., \mathbf{x}_N) = \frac{1}{\sqrt{N!}} \begin{vmatrix} \Psi_1(\mathbf{x}_1) & \Psi_2(\mathbf{x}_1) & \ldots & \Psi_N(\mathbf{x}_1) \\ \Psi_1(\mathbf{x}_2) & \Psi_2(\mathbf{x}_2) & \ldots & \Psi_N(\mathbf{x}_2) \\ \vdots & \vdots & \ddots & \vdots \\ \Psi_1(\mathbf{x}_N) & \Psi_2(\mathbf{x}_N) & \ldots & \Psi_N(\mathbf{x}_N) \end{vmatrix} \tag{2.16}$$

The function $\Psi_k(\mathbf{x}_l)$, as in equation (2.16), should be interpreted as the wavefunction for an electron in state k at the position $\mathbf{x}_l$.

The Hartree-Fock direct and exchange terms

When calculating the matrix element for the Coulomb-repulsion between two electrons the two-particle wavefunction and the two-electron operator $1/\hat{r}_{12} = 1/|\mathbf{r}_1 - \mathbf{r}_2|$ is used. Suppose that the wavefunction for an electron in state one has the position coordinates $\mathbf{x}_1$ and the wavefunction for an electron in state two has the position coordinates $\mathbf{x}_2$, then the matrix element for the interaction between these two electrons becomes

$$\mathbf{V}_{12}^{ee} = \langle \Phi_{12}(\mathbf{x}_1, \mathbf{x}_2) | \frac{1}{\hat{r}_{12}} | \Phi_{12}(\mathbf{x}_1, \mathbf{x}_2) \rangle = \int\int dV_1 dV_2 \left[\Phi_{12}^*(\mathbf{x}_1, \mathbf{x}_2) \frac{1}{|\mathbf{r}_1 - \mathbf{r}_2|} \Phi_{12}(\mathbf{x}_1, \mathbf{x}_2) \right]. \tag{2.17}$$

However by equation (2.16) one knows

$$\Phi_{12}(\mathbf{x}_1, \mathbf{x}_2) = \frac{1}{\sqrt{2}} \left[\Psi_1(\mathbf{x}_1)\Psi_2(\mathbf{x}_2) - \Psi_2(\mathbf{x}_1)\Psi_1(\mathbf{x}_2) \right]. \tag{2.18}$$

Furthermore it is known that

$$\int \left(\Psi_2(\mathbf{x}_1)\Psi_1(\mathbf{x}_2) \frac{1}{\hat{r}_{12}} \Psi_2(\mathbf{x}_1)\Psi_1(\mathbf{x}_2) \right) dV = \int \left(\Psi_1(\mathbf{x}_1)\Psi_2(\mathbf{x}_2) \frac{1}{\hat{r}_{12}} \Psi_1(\mathbf{x}_1)\Psi_2(\mathbf{x}_2) \right) dV \tag{2.19}$$

due to that particle one and two are indistinguishable[5]. The knowledge of equation (2.18) and (2.19) leeds to the matrix element for the electron-electron

[5] Just change the place of particle one and two to get from the left-hand-side to the right-hand-side of equation (2.19)

interaction in a two-electron system

$$\begin{aligned}&\mathbf{V}_{12}^{ee} = \langle\Phi_{12}(\mathbf{x}_1\mathbf{x}_2)|\tfrac{1}{|\mathbf{r}_1-\mathbf{r}_2|}|\Phi_{12}(\mathbf{x}_1\mathbf{x}_2)\rangle = \\ &\int\int dV_1 dV_2\left(\left[\Psi_1(\mathbf{x}_1)\Psi_2(\mathbf{x}_2)\tfrac{1}{\hat{r}_{12}}\Psi_1(\mathbf{x}_1)\Psi_2(\mathbf{x}_2)\right]-\left[\Psi_1(\mathbf{x}_1)\Psi_2(\mathbf{x}_2)\tfrac{1}{\hat{r}_{12}}\Psi_2(\mathbf{x}_1)\Psi_1(\mathbf{x}_2)\right]\right) = \\ &\langle\Psi_1(\mathbf{x}_1)\Psi_2(\mathbf{x}_2)|\tfrac{1}{|\mathbf{r}_1-\mathbf{r}_2|}|\Psi_1(\mathbf{x}_1)\Psi_2(\mathbf{x}_2)\rangle - \langle\Psi_1(\mathbf{x}_1)\Psi_2(\mathbf{x}_2)|\tfrac{1}{|\mathbf{r}_1-\mathbf{r}_2|}|\Psi_2(\mathbf{x}_1)\Psi_1(\mathbf{x}_2)\rangle.\end{aligned} \tag{2.20}$$

If we want to calculate the matrix element of the electron-electron interaction in the *N-electron system* we generalize (2.20) in the following way

$$\begin{aligned}&\langle\Phi_{12\ldots N}(\mathbf{x}_1,\mathbf{x}_2,\ldots,\mathbf{x}_N)|\textstyle\sum_{k<l}^{N}\tfrac{1}{|\mathbf{r}_k-\mathbf{r}_l|}|\Phi_{12\ldots N}(\mathbf{x}_1,\mathbf{x}_2,\ldots,\mathbf{x}_N)\rangle = \sum_{k<l}^{N}\mathbf{V}_{kl}^{ee} = \\ &\sum_{k<l}^{N}\left[\langle\Psi_k(\mathbf{x}_k)\Psi_l(\mathbf{x}_l)|\tfrac{1}{|\mathbf{r}_k-\mathbf{r}_l|}|\Psi_k(\mathbf{x}_k)\Psi_l(\mathbf{x}_l)\rangle - \langle\Psi_k(\mathbf{x}_k)\Psi_l(\mathbf{x}_l)|\tfrac{1}{|\mathbf{r}_k-\mathbf{r}_l|}|\Psi_l(\mathbf{x}_k)\Psi_k(\mathbf{x}_l)\rangle\right] = \\ &\sum_{k<l}^{N}\left(\mathbf{V}_{kl}^{D}-\mathbf{V}_{kl}^{EX}\right).\end{aligned} \tag{2.21}$$

Here $\mathbf{V}_{kl}^{D}$ is called the *Hartree-Fock direct term* or just Hartree term and $\mathbf{V}_{kl}^{EX}$ is called the *Hartree-Fock exchange term*. The exchange term is a consequence of the anti-symmetric many-particle wavefunction and thus is not present for example in the case of interaction between distinguishable particles[6].

Local density exchange

Though equation (2.21) is a beautiful theoretical achievement the Hartree-Fock exchange term can be quite cumbersome and time demanding to use when doing calculations. An alternate way to calculate the exchange term is by so called local density theory.

A complete derivation of this term extends the purpose of this work, however I recommend a well written paper by Slater[7].

He explains that: *with the exchange term one removes from the immediate vicinity of the electron, whose wavefunction one are finding, a exchange charge density whose total amount is just enough to equal a single electronic charge. That is, this corrected charge distribution equals the charge of $n-1$ electrons, as it should.*

The idea of local density exchange is to use an averaged exchange hole for all electrons. The local density exchange term in two dimensions turns out to be[8]

$$V_{ex} = -4a_0^*\sqrt{\frac{2\rho(r)}{\pi}}, \tag{2.22}$$

where a_0^* is the effective Bohr radius and $\rho(r) = \sum_{k=1}^{N}|\psi_k(r)|^2$ is the local electron density.

However, keep in mind, that this is an approximation. Nevertheless there exists a remarkable theorem, the Hohenberg and Kohn theorem[14], which states that an exact representation of the ground state properties of a stationary, nonrelativistic many-particle system in terms of the ground state density is possible. Unfortunately the theorem does not give any clues to how this should be accomplished.

The local density approximation works best for large particle numbers and for equal amounts of spin up and spin down electrons. More extensive and

[6] In the case of boson-boson interaction the sign between the direct and exchange term becomes +.

complicated theories such as *Spin Density*- and *Current Spin Density*-theories and others are available under the framework of *Density Functional Theory* or DFT[14].

2.5.3 Multipole expansion of the inverse radial distance

When working in a central field approximation in atomic physics one expand the inverse radial distance, $1/\hat{r}_{12} = 1/|\mathbf{r}_1 - \mathbf{r}_2|$, in spherical harmonics. This by using a so called multipole expansion[10]. In this way the two-electron operator, $1/\hat{r}_{12}$, becomes a function of the quantum numbers of the wavefunctions it is working on. Here however we have circular symmetry and not spherical as in atomic physics. Cohl et al.[11] suggest an alternate multipole expansion in circular cylindrical coordinates $\mathbf{r} = (R, \phi, z)$,

$$\frac{1}{|\mathbf{r}_1 - \mathbf{r}_2|} = \frac{1}{\pi\sqrt{R_1 R_2}} \sum_{m=-\infty}^{m=\infty} Q_{m-1/2}(\chi) e^{im(\phi_1 - \phi_2)}, \tag{2.23}$$

where $Q_{m-1/2}$ is a Legendre function of the second kind of half-integer degree and

$$\chi = \frac{R_1^2 + R_2^2 + (z_1 - z_2)^2}{2R_1 R_2}. \tag{2.24}$$

Since we have a circular confinement and not a cylindrical one $z_1 = z_2$. So in our case

$$\chi = \frac{R_1^2 + R_2^2}{2R_1 R_2}. \tag{2.25}$$

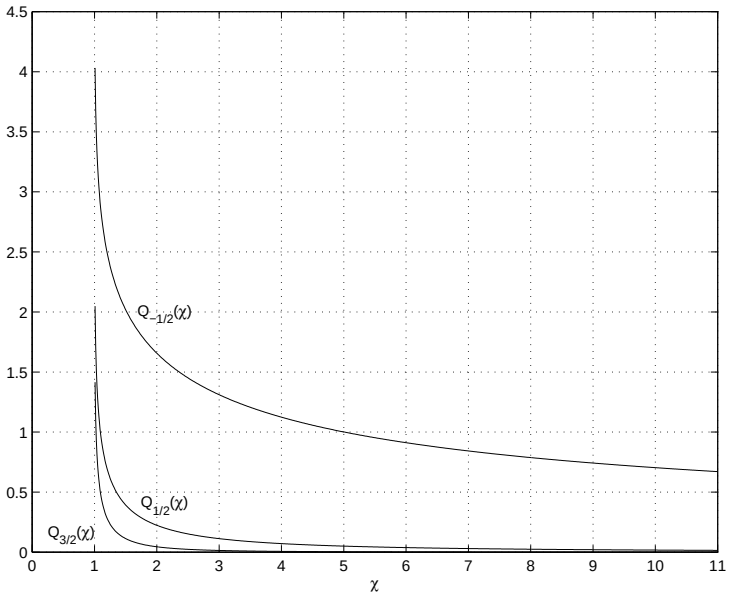

Figure 2.1: *The three toroidal harmonics $Q_{-1/2}$, $Q_{1/2}$ and $Q_{3/2}$ as functions of χ.*

In figure 2.1 the $Q_{m-(1/2)}$–functions with the three lowest possible values of $|m|$ are plotted. The $Q_{m-(1/2)}$–functions are a subgroup of $Q^n_{m-(1/2)}$, i.e. the so called toroidal harmonics[12]. It should be mentioned that the $Q_{m-1/2}$–functions have the property $Q_{m-(1/2)} = Q_{-m-(1/2)}$[11].

The toroidal harmonics have been evaluated using software DTORH1 described in [13].

2.5.4 Conditions for the electron-electron interaction matrix element

What conditions do we get when calculating the electron-electron interaction elements if we have a software that generates the toroidal harmonics? Suppose we are calculating a matrix element of the type $\langle AB|\frac{1}{\hat{r}_{12}}|CD\rangle$. Then we have

$$\langle AB|\frac{1}{\hat{r}_{12}}|CD\rangle = \underbrace{\langle ab|\frac{1}{\hat{r}_{12}}|cd\rangle}_{\text{spatial}}\underbrace{\langle\chi_a|\chi_c\rangle\langle\chi_b|\chi_d\rangle}_{\text{spin}} \tag{2.26}$$

If $\chi_a \neq \chi_c$ or $\chi_b \neq \chi_d$ the element is identically equal to zero. However if the spin parts are non-zero we know by equation (2.23) that the spatial part

$$\langle ab|\frac{1}{\hat{r}_{12}}|cd\rangle = K\int_0^{2\pi}\int_0^{2\pi} d\phi_1 d\phi_2 \left[\sum_{m=-\infty}^{\infty} e^{-im_a\phi_1}e^{-im_b\phi_2}e^{im(\phi_1-\phi_2)}e^{-im_c\phi_1}e^{-im_d\phi_2}\right], \tag{2.27}$$

where K is some constant containing both the radial integral and some constants from the multipole expansion. We see from equation (2.27) that the angular integrals equal zero except when the following conditions are fulfilled:

$$-m_a + m + m_c = -m - m_b + m_d = 0 \Leftrightarrow \begin{cases} m = & m_a - m_c \\ m = & m_d - m_b \end{cases}$$

So if we are calculating an matrix element of the form $\langle AB|\frac{1}{\hat{r}_{12}}|AB\rangle$, that is the Hartree term, we get $\langle\chi_a|\chi_a\rangle = 1$, $\langle\chi_b|\chi_b\rangle = 1$ and $m = 0$ always.

However if we are calculating an matrix element of the form $\langle AB|\frac{1}{\hat{r}_{12}}|BA\rangle$, i.e. the Hartree Fock exchange term, we get $\langle\chi_a|\chi_b\rangle = 1$ and $\langle\chi_b|\chi_a\rangle = 1$ only if state a and b have the same spin and $\langle\chi_a|\chi_b\rangle = 0$ and $\langle\chi_b|\chi_a\rangle = 0$ otherwise. If a and b have the same spin then $m = m_a - m_b$.

2.6 Effects of an external magnetic field in the $\hat{z}$-direction

Experimentally many properties of quantum dots can be seen if an external magnetic field is applied. So what happens theoretically if we do the same?

Let us apply the magnetic field perpendicular to our 2D quantum dot, that is $\mathbf{B} = (0, 0, B)$. We know that the vector potential can be chosen so that

$$\mathbf{A} = \frac{1}{2}(\mathbf{B}\times\mathbf{r}) = \frac{1}{2}(Bx\hat{\mathbf{y}} - yB\hat{\mathbf{x}}). \tag{2.28}$$

Furthermore we know[17] that $\mathbf{p} \rightarrow (\mathbf{p} + \mathbf{A})$ when a magnetic field is applied. This implies that the Hamiltonian

$$\hat{H} = \frac{1}{2}(\mathbf{p} + \mathbf{A})^2 + V = \frac{1}{2}\mathbf{p}^2 + \frac{1}{2}(\mathbf{p} \cdot \mathbf{A} + \mathbf{A} \cdot \mathbf{p}) + \frac{1}{2}\mathbf{A}^2 + V. \tag{2.29}$$

It follows from equation (2.28) that

$$\mathbf{p} \cdot \mathbf{A} = \mathbf{A} \cdot \mathbf{p} = \frac{1}{2}B(xp_y - yp_x) = \frac{1}{2}B\hat{L}_z \tag{2.30}$$

and

$$\mathbf{A}^2 = \frac{1}{4}(Bx\hat{\mathbf{y}} - By\hat{\mathbf{x}})^2 = \frac{1}{4}B^2(x^2 + y^2) = \frac{1}{4}B^2r^2. \tag{2.31}$$

The spin -magnetic field interaction can be included in the following way[18]

$$H_{SB} = g^*\mu_B\hat{S}_z = \frac{1}{2}g^*(m^*/m_e)B\hat{S}_z, \tag{2.32}$$

where $\mu_B = \frac{e\hbar}{2m_e} = \frac{e\hbar m^*}{2m_e m^*}$ which in effective atomic units becomes $\mu_B = \frac{1}{2}(m^*/m_e)$. This due to that a quotient of two values of the same quantity is the same independent of units.

All this gives the total Hamiltonian including the effects of the external magnetic field

$$\hat{H} = \frac{\mathbf{p}^2}{2} + V + \frac{1}{8}B^2r^2 + \frac{1}{2}B\hat{L}_z + \frac{1}{2}g^*(m^*/m_e)B\hat{S}_z. \tag{2.33}$$

Chapter 3

Calculations

3.1 One particle calculations

To start with something easy one can calculate the so called one particle solutions. That is to solve the Schrödinger equation with the Hamilton operator

$$\hat{H} = \frac{1}{2}\left[\frac{\partial^2}{\partial r^2} + \frac{\hat{l}_z^2}{r^2} + \omega^2 r^2\right]. \tag{3.1}$$

One can interpret this in two ways. Either one can say that one neglects the electron-electron interaction or one can say that one calculates which states are available for the first electron about to be injected into the dot. Here the latter interpretation one can argue is the more physical one.

Figure 3.1a) shows the so called shell model for the one particle solutions for a typical value of $\hbar\omega$ and material parameters corresponding to GaAs. One notes that the allowed energy values come in equidistant levels. An analogy of the atomic physics convention of labeling the shells is adopted. This convention is that the first number is the principal quantum number, also called the radial quantum number. After that comes a letter where s=0, p=1, d=2, f=3, g=4 and so on. This letter corresponds here to the absolute value of the angular quantum number. One significant difference between the labeling in atomic physics and that adopted here is that in atomic physics the letter corresponds to the angular momentum quantum number l, i.e the length of the angular momentum vector, but here it corresponds to $|m_l|$, i.e the absolute value of the projection of the angular momentum vector on the chosen axis[1]. The reason for this difference is that in the 2D quantum dot case there only exists one orbital quantum number, m_l, while in the atomic case two orbital quantum numbers, l and m_l, exist.

For a given shell in a 2D quantum dot one can only obtain two values of the angular quantum number, $+|m_l|$ and $-|m_l|$. For the s-shells this means that in the quantum dot case as well as in the atomic case only two states, one with spin up and the other with spin down, are possible. For the other shells things differ in the atomic and quantum dot cases. In the atomic case $2(2l+1)$ different states are possible[2] but in the quantum dot case only 4 different states

[1] Elsewhere in this report m_l is denoted m.

[2] The $2l+1$ term is for $m_l = l, l-1, \ldots, -l$ multiplied with 2 for the spin up and spin down cases.

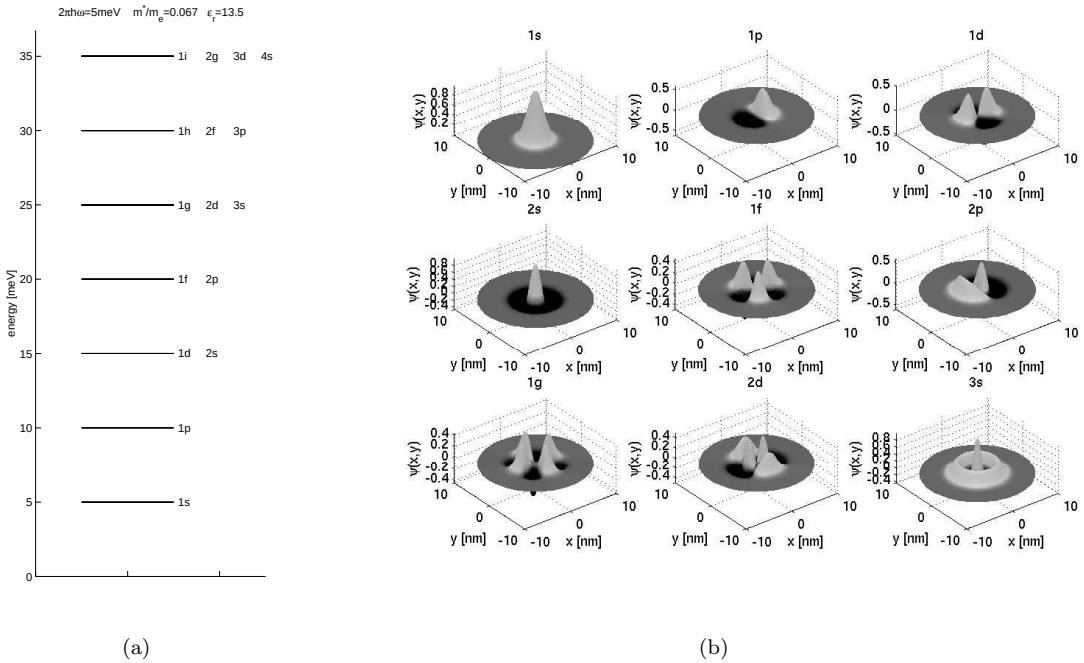

(a) (b)

Figure 3.1: *a) Shell model for the one particle solutions calculated with material parameters corresponding to GaAs. b) The real part of the nine least energetic one particle wavefunctions in a).*

are possible[3] independent of which shell it is as long as it is not a s-shell.

Furthermore one notices that with the one particle solutions high degeneracy is possible. Not only electrons in the same shell share energy value but also electrons from different shells according to figure 3.1a). However when the electron-electron interaction is taken into account the energy levels split due to the electrons mutual Coulomb repulsion.

One also sees that a different order of the shells appear in these 2D quantum dots than in the atomic case. In atomic physics the order of the shells is $1s, 2s, 2p, 3s, 3p, \ldots$ but here the order is $1s, 1p, 1d$-$2s$,$1f$-$2p, \ldots$. Here x-y denotes that shell x and y are degenerate.

In figure 3.1b) the real part of some one particle wavefunctions are plotted. In the atomic case a plot of the wavefunctions is not possible, at least not all axis at once, because atoms of course are three dimensional[4]. One notices that all s-wavefunctions are circular symmetric. This is not the case for the non s-shell wavefunctions. However it is clear if one where to calculate the probability density, $|\psi|^2$, it would be circular symmetric.

[3] Two (one spin up and one down) for $-|m|$ and two for $+|m|$.

[4] This requires four axis; the three space coordinates plus the probability amplitude. The probability amplitude can in that case be represented with for example different shadings or colors.

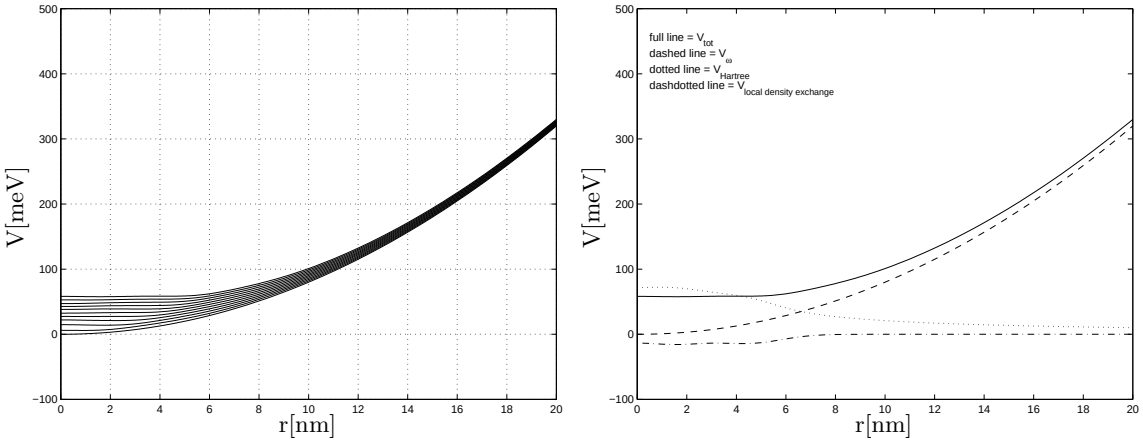

(a) (b)

Figure 3.2: *a) The effective potentials for the* $1, 2, 4, 6, \ldots, 20$*th electrons according to local density calculations. b) The different parts of the total potential for the 20:th electron according to local density calculations. The parameters used for the calculations in both a) and b) are* $\hbar\omega = 4meV$, $m*/m_e = 0.067$, $\epsilon_r = 13.5$.

3.2 Many particle calculations

3.2.1 local density calculations

Now it is time to include the electron-electron interaction. We start this by using the local density calculations mentioned in section 2.5.2 on page 13. Hence the Hamilton operator becomes

$$\hat{H} = \frac{1}{2}\left[\frac{\partial^2}{\partial r_1^2} + \frac{\hat{l}_z^2}{r_1^2}\right] + \underbrace{\frac{1}{2}\omega^2 r_1^2}_{V_\omega} + \underbrace{\sum_{k=1}^{N}\int dr_2 \frac{|\psi_k(r_2)|^2}{|\mathbf{r}_1 - \mathbf{r}_2|}}_{V_H} - \underbrace{4\sqrt{\frac{2\rho(r_1)}{\pi}}}_{V_{ldex}}, \qquad (3.2)$$

where r_1 is the radial coordinate of the matrix element integration and r_2 the radial coordinate of the Hartree term integration.

Here the term in the square bracket is the radial equation for circular coordinates, the second term (V_ω) is the harmonic potential from the surrounding, the third term (V_H) is the Hartree Fock direct term[5] and the last term (V_{ldex}) is the local density exchange term.

The effective potential and its constituents

To get a more intuitive picture of what the effect of all these potentials really becomes study figure 3.2a). It shows the self consistent effective potentials, $V_{eff} = V_\omega + V_H + V_{ldex}$, for the $1, 2, 4, 6, \ldots, 20$th electron. One clearly sees

[5] or just Hartree term

how the effective potential builds up in the bottom of the well and flattens out with increasing particle number. This is due to the electrons mutual Coulomb repulsion.

The next question one asks oneself is in what way do these different potentials build up the effective potential? Figure 3.2b) shows the self consistent effective potential and its different constituents for the 20th electron. To the surrounding harmonic potential (V_ω) one adds the Hartree term (V_H) i.e. the Coulomb repulsion. However the Hartree term is reduced by the local density exchange term (V_{ldex}). The exchange term somehow takes into account that the electrons do not act on themselves. This can be interpreted as if an exchange hole is produced by the electrons which lowers the potential or as a positive charge distribution that screens of some the interaction between the electrons.

Chemical potential, addition energy and shell structure

The chemical potential for the N-particle system is simply defined as

$$\mu(N) = E(N) - E(N-1), \tag{3.3}$$

where $E(N)$ is the total energy of the N-particle system. That is the chemical potential for the N-particle system corresponds to the energy it costs to inject the N:th electron into the system[6].

To calculate the chemical potential the total energy $E(N)$ of the N-particle system must first be calculated. This can *not* be done by just adding the orbital energies, ϵ_i, because the electron-electron interaction will then be counted twice. This is perhaps best illustrated by an example. If one where to calculate for example $E(2)$, that is the total energy of the two particle system one might naively just sum the orbital energies, ϵ_1 and ϵ_2. However

$$\epsilon_1 = \epsilon_{\omega 1} + \underbrace{\langle\psi_1\psi_2|\frac{1}{\hat{r}_{12}}|\psi_1\psi_2\rangle - \langle\psi_1\psi_2|\frac{1}{\hat{r}_{12}}|\psi_2\psi_1\rangle}_{\epsilon_{12}} \tag{3.4}$$

and

$$\epsilon_2 = \epsilon_{\omega 2} + \underbrace{\langle\psi_2\psi_1|\frac{1}{\hat{r}_{12}}|\psi_2\psi_1\rangle - \langle\psi_2\psi_1|\frac{1}{\hat{r}_{12}}|\psi_1\psi_2\rangle}_{\epsilon_{21}}, \tag{3.5}$$

where $\epsilon_{\omega 1}$ and $\epsilon_{\omega 2}$ are the energies of the one electron states which electron one and two possess respectively[7]. This implies that if one adds ϵ_1 and ϵ_2 the interaction will be counted twice[8] and this is not correct. A way to handle this is to subtract half of the interaction part of each ϵ_i when adding the orbital energies. That is

$$E(2) = \epsilon_1 - \frac{1}{2}\epsilon_{12} + \epsilon_2 - \frac{1}{2}\epsilon_{21}. \tag{3.6}$$

Generalizing this to the N-particle system yields

$$E(N) = \sum_{i=1}^{N}\left[\epsilon_i - \frac{1}{2}\sum_{j=1}^{N}\epsilon_{ij}\right]. \tag{3.7}$$

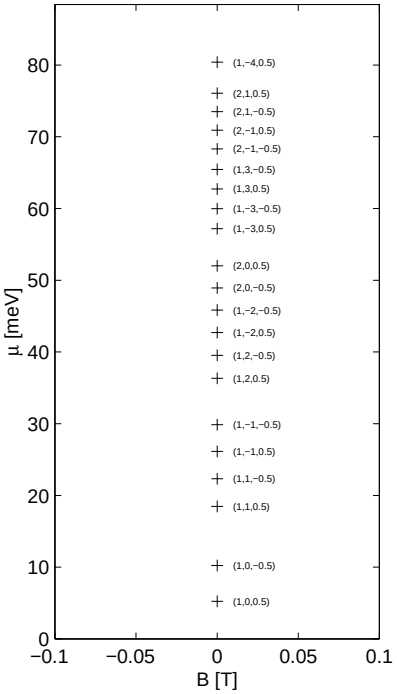

Figure 3.3: *Chemical potentials for the 1st,2nd,. . . ,21 ground state electron systems according to self consistent local density calculations. The states are labeled according to the notation* (n, m_l, m_s). *The parameters used are* $\hbar\omega = 5meV$, $m*/m_e = 0.067$, $\epsilon_r = 13.5$.

When one knows how to calculate total energy the calculation of the chemical potential is trivial by equation (3.3).

Figure 3.3 shows the chemical potential for the first 21 electron systems according to local density calculations. It illustrates an example of what ground state configuration local density calculations leed to. However it should here be mentioned that the local density method does not differ between $m_l = -|m_l|$ and $m_l = +|m_l|$ or between $m_s = -\frac{1}{2}$ and $m_s = \frac{1}{2}$. That is the same total energy would have been obtained for example with the third electron in states $(n, m_l, m_s) = (1, \pm 1, \pm 0.5)$. This is a weakness of the local density theory because even without magnetic fields the interaction between electrons will in reality depend on their spin through the Pauli exclusion principle.

Furthermore figure 3.3 depicts some sort of shell structure. This becomes clearer when studying figure 3.4. It shows the so called addition energy as a function of particle number for four different potentials. The addition energy is defined as

$$\Delta_N = \mu(N+1) - \mu(N). \tag{3.8}$$

[6]This corresponds to the ionization energy in atomic physics.

[7]The exchange term is here written as the Hartree-Fock exchange term but the problem of double counting remains the same when using local density exchange.

[8]Note that $\epsilon_{12} = \epsilon_{21}$ due to that electrons are indistinguishable.

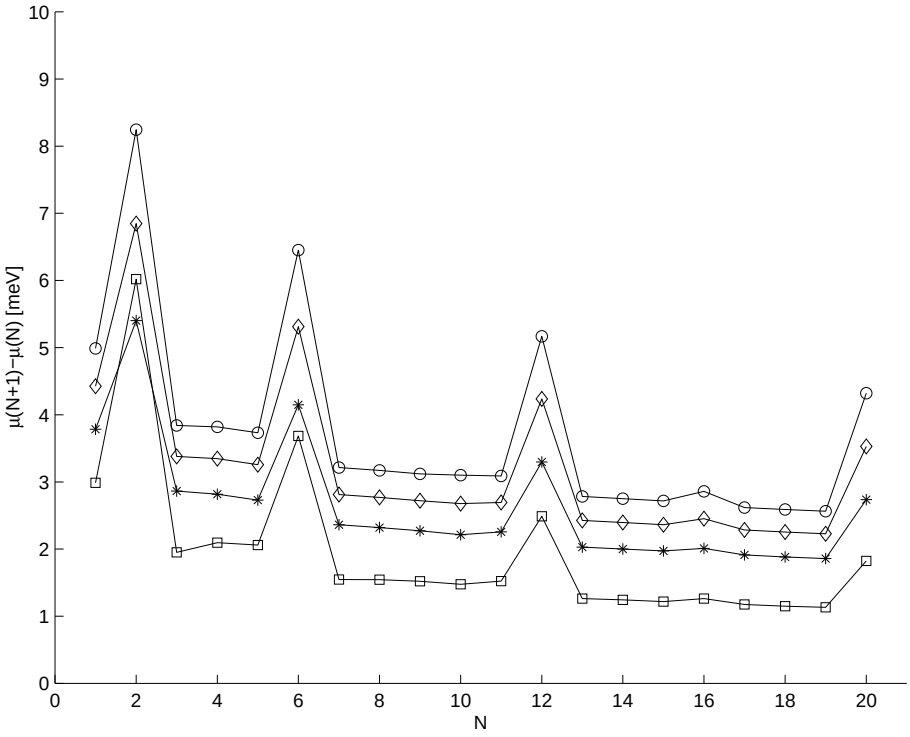

Figure 3.4: *Addition energy as a function of particle number for local density calculations with four different potentials. The curve labeled with ∘ has been calculated with $\hbar\omega = 5meV$, the curve labeled with ♢ has been calculated with $\hbar\omega = 4meV$, the curve labeled with * has been calculated with $\hbar\omega = 3meV$, and the curve labeled with □ has been calculated with $\omega^2 = \frac{e^2}{4\pi\epsilon\epsilon_r m^* r_s^3\sqrt{N}}$ and $r_s = 1.51a_B^*$, as discussed in the text. For all four calculations the material parameters used where $m*/m_e = 0.067$ and $\epsilon_r = 13.5$ corresponding to GaAs.*

That is Δ_N is the difference in how much energy it costs to inject the next particle into the system compared to the last.

Here the shell structure becomes apparent. Clear magic shells form at the particle numbers $N = 2, 6, 12, 20$. A weak subshell is indicated at $N = 16$.

In an experiment done by Tarucha et. al.[1] the addition energy as a function of particle number in a vertical quantum dot was measured. The results of the measurements are plotted in figure 3.5. When comparing this addition energy spectra to the one in figure 3.4 both similarities and differences in the results appear. First of all, peaks occur for the same particle numbers. This is of course a very important result because we now can say that we have shown the shell structure of the 2D circular quantum dot. Furthermore one sees that in figure 3.5 the peaks in the addition energy spectra get less and less distinct as the particle number increases to the extent that the $N = 20$ peak vanishes. This is of course due to that the most energetic electrons start to interact with the surrounding material. This is not accounted for in our

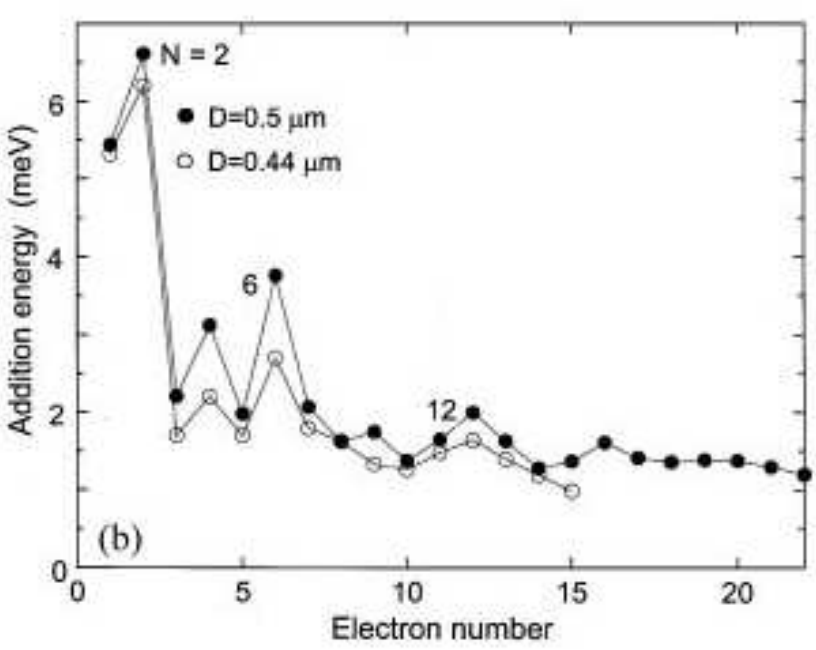

Figure 3.5: *Addition energy spectra from Tarucha et al.:s[1] experiment.*

model so it is no surprise that this differs. Macucci et. al. [9] included this in their calculation by applying a method including image charges with the expected result; the addition energy spectra did flatten out with increasing particle number. Moreover we see that the calculations with constant $\hbar\omega$ with reasonable value[9] gives a too large addition energy for all particle numbers. Reimann and Manninen [20] argues that:

Experimentally, however, if one makes the voltage on (the side or top) gates less negative, the effective confinement strength ω decreases. At the same time, the number of electrons in the dot increases. Thus we may also consider keeping the average electron density in the dot constant, i.e., fixing the density parameter r_s and varying ω with N. Indeed, for vertical dots it turns out that as N increases, the confinement weakens so that the particle density tends to a constant [21].

Koskinen et. al. [22] suggests a way to handle this by approximating ω with

$$\omega^2 = \frac{e^2}{4\pi\epsilon\epsilon_r m^* r_s^3 \sqrt{N}}, \tag{3.9}$$

where r_s is the 2D Wigner-Seitz radius depending on the average particle density ρ_0 by $\rho_0 = 1/(\pi r_s^2)$. This is what has been used in the calculation of the curve marked with $\square$ in figure 3.4 with $r_s = 1.51a^*$ corresponding to the equilibrium density of the 2D electron gas. One sees that the wished for effect occurs when the addition energy for all particle numbers decreases and flattens out without decreasing the values of the first peaks too much.

[9] In section 3.3.1 on page 27 it will become more clear what values of $\hbar\omega$ is reasonable.

Moreover the experimental result gives a much more rugged addition energy spectra, at least for small particle numbers, than the local density calculations do. For example the $N = 4$ peak in the experimental addition energy spectra does not show up at all in the local density calculation. This is simply a consequence of that local density does not differ between spin up and down and hence energy splittings due to spin effects do not occur in zero magnetic field.

3.2.2 Hartree-Fock calculations

For an alternate description of the electron-electron interaction in the dot spin-polarized Hartree-Fock calculations have been performed. That is the Hartree-Fock exchange matrix element

$$\sum_{ij} V_{ij}^{ex} = \sum_{ij} \langle \psi_i(\mathbf{x}_i)\psi_j(\mathbf{x}_j)|\frac{1}{r_{ij}}|\psi_j(\mathbf{x}_i)\psi_i(\mathbf{x}_j)\rangle \tag{3.10}$$

is used for the exchange interaction.

Note that this exchange term implies that the radial functions becomes spin dependent through the Pauli principle as explained in section 2.5.4 on page 15. This is the reason why the name spin-polarized Hartree-Fock is used.

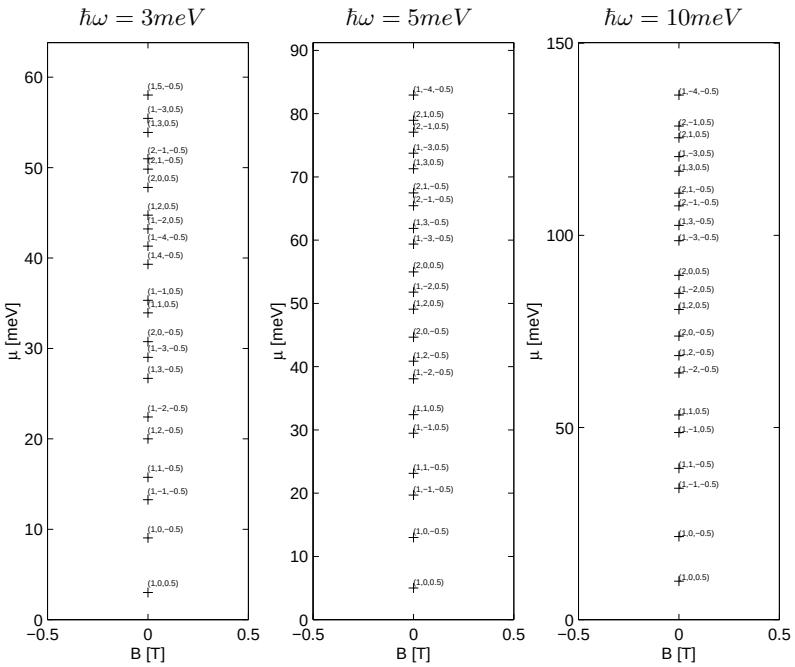

Figure 3.6: *Chemical potentials for the* $1, 2, 3, \ldots, 21$ *ground state electron systems for three different effective confinement strengths according to self consistent spin-polarized Hartree-Fock calculations. The states are labeled according to the notation* (n, m_l, m_s)*. The material parameters used where* $m*/m_e = 0.067$*,* $\epsilon_r = 13.5$ *corresponding to GaAs.*

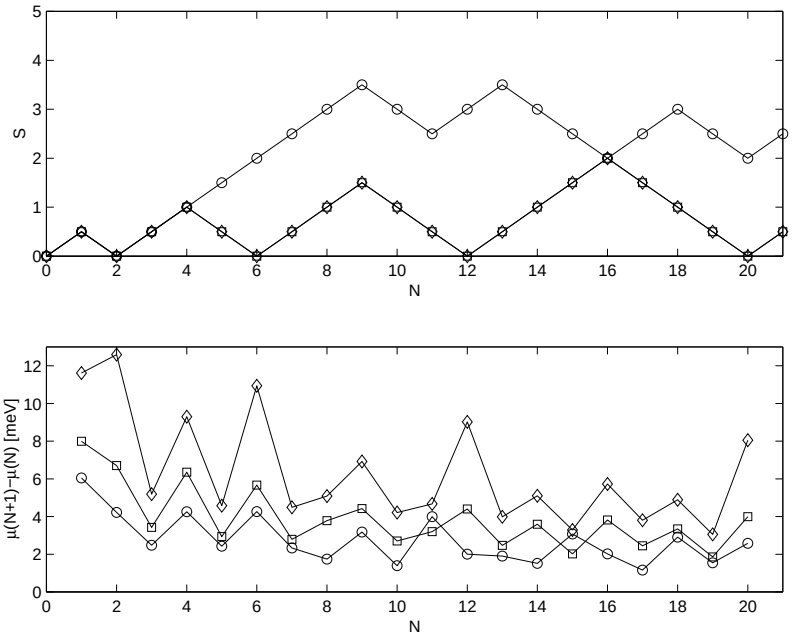

Figure 3.7: *Total spin and addition energy as functions of particle numbers by Hartree-Fock calculations. The curves plotted with ∘ have been calculated with $\hbar\omega = 3meV$, the curves plotted with □ have been calculated with $\hbar\omega = 5meV$ and the and the curves plotted with ⋄ have $\hbar\omega = 10meV$. Upper panel: The total spin S as a function of particle number for three different effective confinement strengths. Closed shells indicated by $S = 0$ show at $N = 2, 6, 12$ and 20 for the two stronger confinements. Lower panel: Addition energy as a function of particle number for Hartree-Fock calculations for three different values of ω. The material parameters used in the calculations where $m*/m_e = 0.067$ and $\epsilon_r = 13.5$ corresponding to GaAs.*

Intuitively one expects better results with Hartree-Fock calculations than with local density calculations because the derivation of the exchange term is more straight forward in the Hartree-Fock case than in the local density case, and in some sense the local density theory is an approximation of the Hartree-Fock theory.

Moreover the spin-polarized Hartree-Fock calculations include spin effects through the exchange term that favors spins of the same kind by lowering the energy. This should generate structure in between closed shells, something that the local density approximation fails to show.

Figure 3.6 shows the chemical potential for the $1, 2, 3, \ldots, 21$ ground state electron systems for three different effective confinement strengths ω. One sees that the configurations differ between the calculation with the lowest value of ω and the two calculations with the greater values of ω. For example, in the calculation with $\hbar\omega = 3$meV, the fifth electron to be injected into the system chooses the $(n, m_l, m_s) = (1, 2, -0.5)$ state but in the calculations with $\hbar\omega = 5$meV and $\hbar\omega = 10$meV the fifth electron chooses the $(1, -1, 0.5)$ state. The reason for this

difference is that in the case of the weaker potential, the exchange term lowers the energy more due to the fact that the $(1, 2, -0.5)$ state has the same spin as three of the previously injected electrons than the m_l^2 term in equation 2.13 raises the energy. However if the potential is increased the electrons choose a more true 2D-harmonic oscillator configuration, that is for every closed shell[10], the same states have been occupied as in the local density approach. The phenomena of different electron configurations for different confinement strengths is well known in atomic physics. Ions with the same number of electrons but with different Z will have different configurations.

Figure 3.7 shows the addition energy and the total spin, S, as functions of particle numbers according to spin-polarized Hartree-Fock calculations. It becomes clear by the upper panel that the calculation with $\hbar\omega = 3$meV fails to show the shell structure with closed shells at $N = 6, 12$ and 20 because $S \neq 0$. However the calculations with the two greater values of ω have $S = 0$ (and $\mathcal{M} = \sum m_l = 0$, see figure 3.6) at $N = 2, 6, 12$ and 20. Thus the Hartree-Fock calculations are able to manifest the shell structure through the electron configuration scheme.

In the lower panel of 3.7 the shell structure is also shown by peaks in the addition energy spectra at $N = 2, 6, 12$ and 20 at least in the $\hbar\omega = 10$meV calculation. This is however a very strong confinement strength. This reflects in that the ground state energies in this calculation become too large when compared with the experimental result. However the shape of the addition energy spectra closely resembles the experimental one.

One also sees by the upper panel in figure 3.7 that the shell filling procedure follows Hund's first rule; that is, it tries to find the maximal total spin while filling the shells. This gives subpeaks in the addition energy spectra (the lower panel) at half-filled shells, at $N = 1, 4, 9$ and 16, due to that it costs more energy to put in an electron with a different spin than it costs to put in an electron of the same spin[11].

3.3 Calculations including effects of an external magnetic field

Let us now consider what happens if we apply an external magnetic field in the z-direction to our 2D quantum dot.

3.3.1 One particle solutions when applying an external magnetic field

At first it is suitable to calculate in what way the one particle solutions depend on the field. We know by equations (3.1) and (2.33) that the Hamilton operator becomes

$$\hat{H} = \frac{1}{2}\left[\frac{\partial^2}{\partial r^2} + \frac{\hat{L}_z^2}{r^2} + \left(\omega^2 + \frac{1}{4}B^2\right)r^2\right] + \frac{1}{2}B\hat{L}_z + \frac{1}{2}g^*(m^*/m_e)B\hat{S}_z. \quad (3.11)$$

[10] A shell is considered closed if the total angular momentum $\mathcal{M} = \sum m_l = 0$ and total spin S=0.

[11] This due to the fact that the exchange term that lowers the energy is non-zero only between particles with the same spin. See page 15 section 2.5.4.

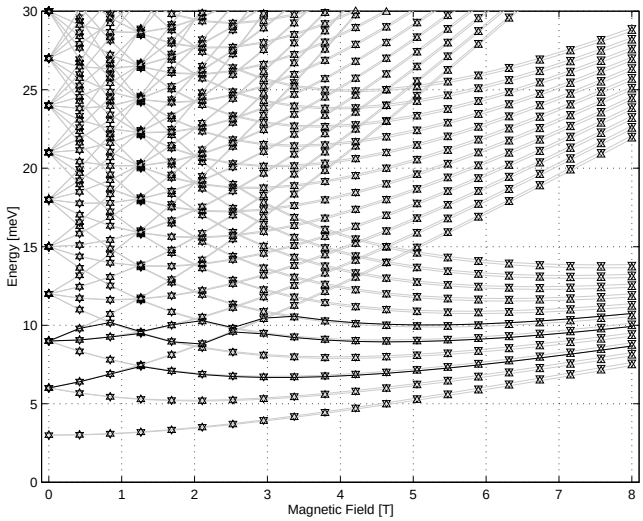

Figure 3.8: *Energy splitting of the one particle energy levels into so called Landau bands due to an external magnetic field. These kind of spectra are usually called Fock-Darwin energy spectra. The states plotted are the ones corresponding to quantum numbers* $n = 1, 2, 3, 4$, $m_l = -10, -9, -8, \ldots, 10$ *and* $m_s = -\frac{1}{2}, \frac{1}{2}$. *Spin up states are labeled with* $\triangle$ *and spin down with* $\bigtriangledown$. *The* $5th$, $9th$ *and* $12th$ *lowest states are highlighted. The effective confinement strength* $\hbar\omega = 4meV$ *and the material parameters* $m* /m_e = 0.067$, $\epsilon_r = 13.5$ *and* $g* = -0.44$ *corresponding to GaAs have been used.*

One concludes that the degenerate energy levels in figure 3.1a) will split due to the coupling of the orbital angular momenta and spin angular momenta with the external magnetic field. This becomes hands on when studying figure 3.8 where the energy levels split into so called *Landau bands*. In high magnetic field one perceive that only states from the lowest Landau band corresponding to $m_l = 0, -1, -2, -3, \ldots$ will be occupied.

Furthermore, as figure 3.8 depicts, the splitting due to the orbital angular momenta coupling to the magnetic field is considerably larger than the splitting due to the spin angular momenta coupling to the magnetic field. This can also be seen from equation (3.11). Typical values of the effective mass is $m^*/m_e \approx 0.067$ and of the g-factor $g^* \approx -0.44$ corresponding to GaAs. This implies that the splitting due to the spin angular momenta coupling with the magnetic field is in the order of a few percent of the orbital angular momenta coupling to the magnetic field.

In figure 3.8 the 5th, 9th and 12th lowest states are highlighted. This enhances that the fifth electron to be injected into the system will switch states at approximately 1.2T and in the same way the 9th electron switches states three times at approximately 1.2, 2 and 2.5T before settling into the lowest Landau band. This state switching will produce a wiggling motion of the chemical potentials when doing many particle calculations. One can easily imagine that more states will be switched for larger particle numbers when the magnetic field is varied.

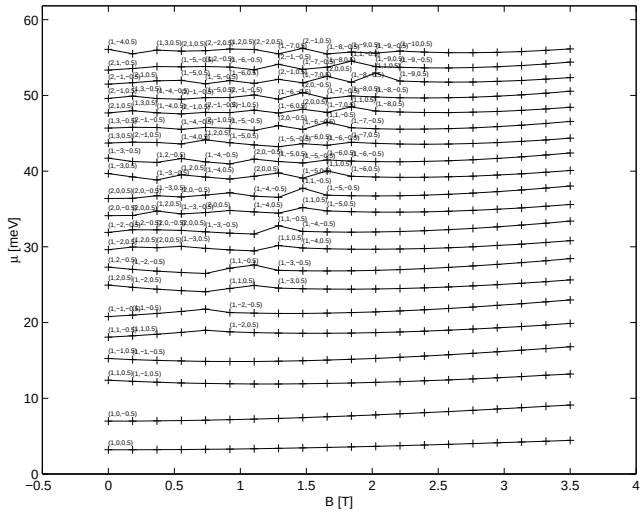

(a) $\hbar\omega = 3\text{meV}$

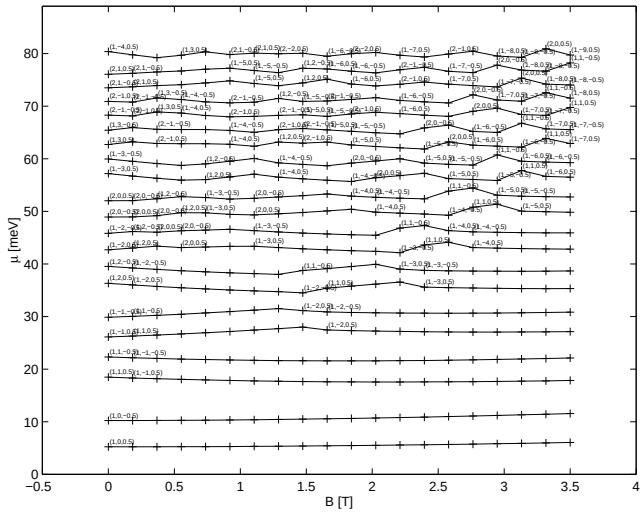

(b) $\hbar\omega = 5meV$

Figure 3.9: *Chemical potentials for the* $1, 2, \ldots, 21$ *ground state electron systems as functions of the magnetic field according to local density calculations for two different effective confinement strengths. When an electron switches states the new state is printed out according to the notation* (n, m_l, m_s)*. The material parameters* $m*/m_e = 0.067$*,* $\epsilon_r = 13.5$ *and* $g* = -0.44$ *corresponding to GaAs.*

3.3.2 Local density calculations including an external magnetic field

What effect will many-particle calculations have on the Fock-Darwin energy spectra [12]?

Figure 3.9 shows the chemical potentials for the $1, 2, \ldots, 21$ ground state electron systems as functions of the magnetic field for two different confinement strengths.

While the first four chemical potentials follow smooth paths when the magnetic field increases the $5, 6, \ldots, 21$ electron chemical potentials wiggles as the corresponding electrons switch states when the magnetic field is varied. For example for $\hbar\omega = 5$meV the fifth and sixth electrons change states at $1 \leq B \leq 1.5$T as the Fock-Darwin spectra predicted. Moreover one sees that the chemical potentials follow each other in pairs corresponding to spin up and spin down electrons of a given m_l.

One also notices that for a given N when the magnetic field reaches a certain value only the lowest Landau band will be occupied and the wiggling stops. Fur-

[12] That is figure 3.8.

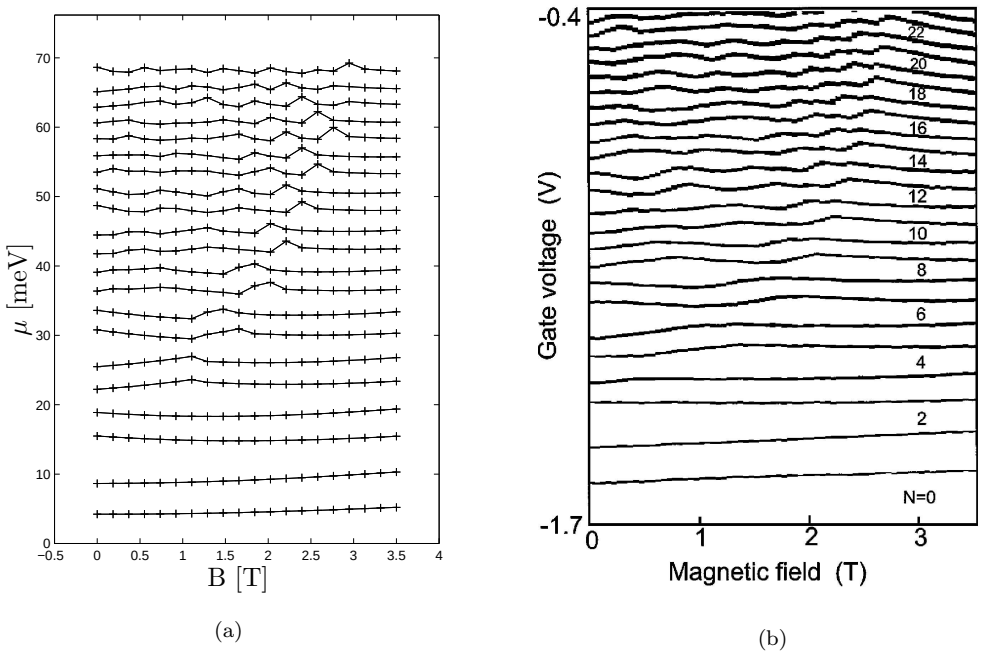

(a) (b)

Figure 3.10: *a) Chemical potentials for the* $1, 2, \ldots, 21$ *ground state electron systems as functions of the magnetic field according to local density calculations. The effective confinement strength* $\hbar\omega = 4meV$ *and the material parameters* $m*/m_e = 0.067$, $\epsilon_r = 13.5$ *and* $g* = -0.44$ *corresponding to GaAs where used. b) Evolution of the peak positions (voltages) of the Coulomb blockade oscillations with magnetic field according to Tarucha et al:s[1] experiment. The particle numbers* N *are indicated at respective Coulomb peak.*

thermore one observe a significant difference in for what magnetic field strengths the transitions to the Landau band occur between the two calculations.

In figure 3.10a) $\hbar\omega = 4$meV has been used. Figure 3.10b) shows the evolution of the peak positions of the Coulomb blockade oscillations from Tarucha et. al.:s[1] experiment. A remarkable similarity between figure 3.10a) and b) is apparent. The wiggling behavior, the pairing of the chemical potentials and the transition to the lowest Landau band are all seen in both figures. Furthermore if one compares the two pictures one can almost identify every wiggle of the chemical potentials. However, some wiggles are not seen, for example the $N = 4$ and 5 systems seem to change states at $B \approx 0.4$T and some pairs even seem to get out of phase with respect to the wiggles in the experiment. These phenomena are not seen at all in the local density calculations but will be explained by the spin-polarized Hartree-Fock calculations. The good agreement between the peak positions in this theoretical and the experimental figures leed to the conclusion that the choice of $\hbar\omega = 4$meV is reasonable.

Figure 3.11 shows addition energy as a function of particle number and magnetic field. Here the wiggling of the states for low magnetic fields and the settling into the lowest Landau band at high magnetic fields becomes obvious.

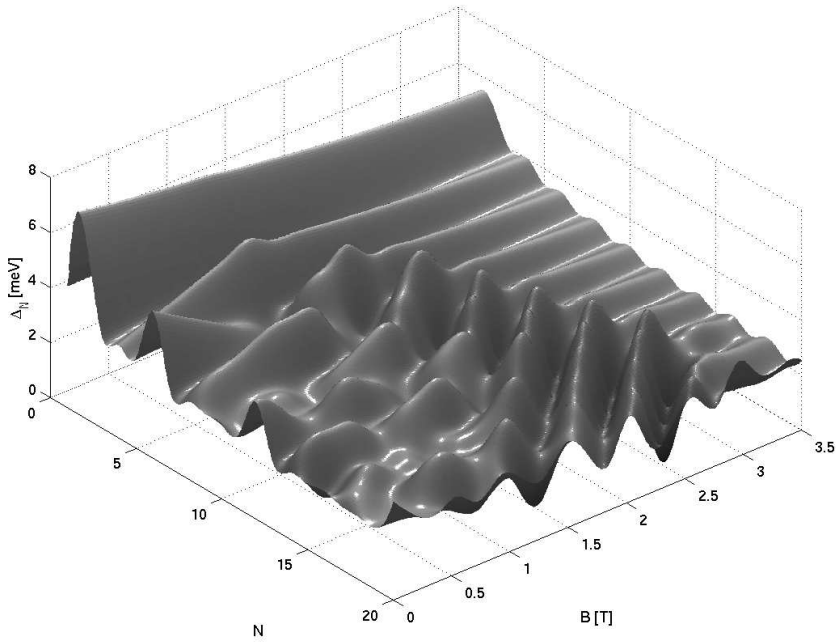

Figure 3.11: *Addition energy, Δ_N, as a function of particle number and magnetic field according to local density calculations with $\hbar\omega = 4meV$. The figure has been generated in MATLAB using interpolation routines to smooth things out and therefore the figure should be interpreted quantitatively and data points should not be taken direct from the figure.*

3.3.3 Hartree-Fock calculations including effects of an external magnetic field

So will Hartree-Fock calculations be able to explain anything that the local density approach fails too?

Figure 3.12 shows the chemical potentials for the $1, 2, 3, \ldots, 10$ electron systems as functions of the magnetic field according to spin-polarized Hartree-Fock calculations.

When comparing this result to figure 3.10b) one first observes that larger magnetic fields are needed to start the wiggling process in the calculated plot compared to the experimental one. This is just because our choice of confinement strength, $\hbar\omega$, is very large compared to the one found reasonable by the local density calculations. However by figure 3.7 on page 25 one concludes that such a strong confinement strength is necessary to get a correct addition energy spectra.

Nevertheless, if we concentrate on the pattern produced by the Hartree-Fock calculations we see that it can explain several wiggles that the local density calculations fails to. For example, in the Hartree-Fock calculations as well as in the experimental result, the $N = 4$ chemical potential starts off (in low magnetic fields) with a positive slope and the in the same way $N = 5$ chemical potential start off with a negative slope. This is something that the local density approximation fails to explain. Why is this?

In the local density case as soon as the magnetic field is switched on the $(1, -1, -0.5)$ state is chosen for the fourth electron. However in the Hartree-Fock case it is energetically favorable to put electron four in state $(1, 1, 0.5)$ due to that the exchange term lowers the energy more than the coupling of the orbital angular momentum to the magnetic field lowers the energy. The $(1, 1, -0.5)$ state then is occupied by the fifth electron. When the magnetic field is increased to a certain extent the fourth electrons orbital angular momenta coupling to the magnetic field lowers the energy more than the exchange does so the fourth electron change state to $(1, -1, -0.5)$ and the fifth electron gets stuck with the $(1, 1, 0.5)$ state.

Moreover one notices that for $N > 5$ wiggles seem to appear in the Hartree-Fock calculations that are not seen in the experimental result. This can be due to two reasons.

The first reason would be that the resolution in the experimental results seem to be quite bad[13], at least compared with what a calculation resolves. So maybe the calculation can resolve what the experiment cannot? This standpoint is enhanced by the fact that Steffens et. al.[23] used a current spin density approach and came up with a similar wiggling procedure to this Hartree-Fock calculation[14]. Several authors, [24][25] and more, used Hartree-Fock calculations to generate plots of chemical potentials as functions of the magnetic field. However in [24] the dielectric constant was altered to get a good agreement with Tarucha et. al.s experiment and in [25] the switchings occur for much stronger magnetic fields than in Tarucha et. al.s experiment. Still these Hartree-Fock calculations show similar state switching as those found in our calculation.

The other reason is that since the effective confinement strength is so large some state switching can occur that does not happen in the experiment. If this

[13] For this conclusion one must study Tarucha et.al.:s article [1].

[14] However they could use a more reasonable effective confinement strength.

is true the only way to check it would to be to extend our theory in some way so that the wiggle positions of figure 3.12 and the ground state energies would correspond better to the experimental result without altering the shape of the ground state addition energy spectra of figure 3.7 on page 25 too much.

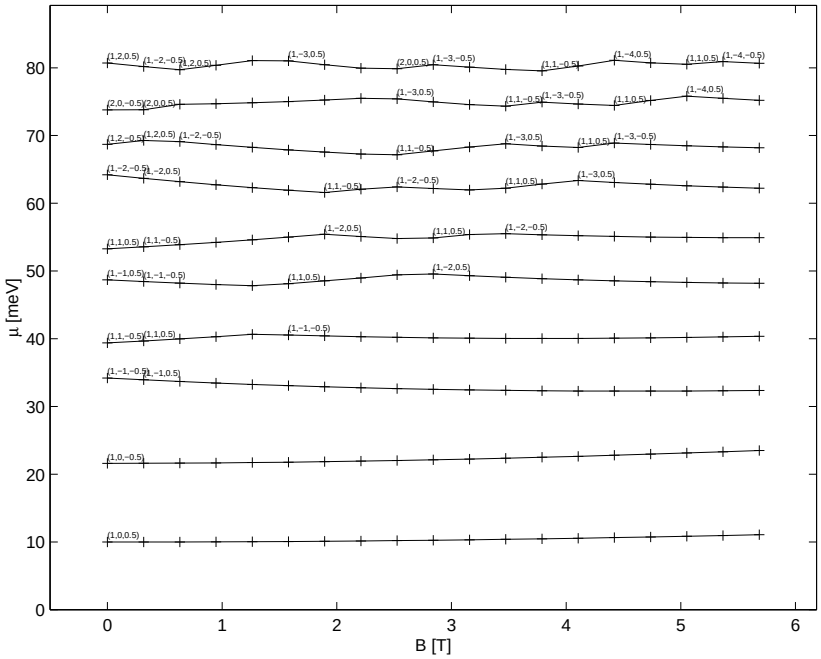

Figure 3.12: *Chemical potentials for the* $1, 2, 3, \ldots, 10$ *electron systems as functions of the magnetic field according to spin-polarized Hartree-Fock calculations with* $\hbar\omega = 10meV$*. When an electron has changed states it is indicated by printing out the new state according to the notation* (n, m_l, m_s)*. The material parameters* $m*/m_e = 0.067$*,* $\epsilon_r = 13.5$ *and* $g* = -0.44$ *corresponding to GaAs where used.*

Chapter 4

Summary and Conclusions

The *mean-field approximation* where each electron moves independently of the other electrons in a circular symmetric field produced by the surroundings and the other electrons can describe many properties of *two dimensional circular quantum dots* very well.

The *local density approximation* as well as the *spin-polarized Hartree-Fock approximation* predicts the shell structure in *2D circular quantum dots*, with magic shells at $N = 2, 6, 12, 20$. The shells can be seen by peaks in the addition energy spectra for these particle numbers.

Even though the *local density approximation* fails to show the structure in between closed shells the *spin-polarized Hartree-Fock* approximation succeeds in doing this. This difference is due to that the *spin-polarized Hartree-Fock* calculations have a spin dependent exchange interaction while the *local density exchange* is spin independent. However if the effective confinement strength is too small the spin-exchange effects take over. It turns out that an unreasonable strong confinement is needed in the *spin polarized Hartree-Fock* calculations to get an addition energy spectra that resembles experimental results. With this strong effective confinement strength the *spin-polarized Hartree-Fock calculations* generates too large ground state energies. Nevertheless for such strong confinement strengths the shell filling follow *Hund's first rule* and the calculations succeed in predicting the shell structure through the electron-configuration scheme (as they did through the addition spectra). That is at $N = 2, 6, 12, 20$ both the total orbital angular momenta and the total spin angular momenta equal zero.

Moreover the behavior of a *two dimensional circular quantum dot* in an external magnetic field is described surprisingly well by *local density* calculations. A plot of the chemical potentials as functions of the magnetic field depicts three clear phenomena. The first phenomena is that the electrons switch states as the magnetic field is varied, the second is that the chemical potentials follow each other in pairs corresponding to spin up and spin down of the same m_l and the third is that for a given N as the magnetic field reach a certain limit the electron will choose a state in the lowest *Landau band*. This plot of the chemical potentials as functions of the magnetic field corresponds well to an experimental data if an effective confinement strength $\hbar\omega = 4$meV is chosen for the calculations. The experimental data is in form of a plot of the evolution of the peak positions in the Coulomb blockade oscillations with magnetic field in Tarucha et. al.s

experiment[1]. However some state transitions visible in the experiment are not seen in the local density calculations. These state transitions are explained by the *spin-polarized Hartree-Fock* calculations and thus they are consequences of the spin dependent exchange interaction.

Still here the problem with a too strong confinement strength becomes apparent in the sense that the state transitions take place for much stronger magnetic fields than in the experiment. This problem could in principle be solved by increasing the dielectric constant as in [24][26] but for yours truly this seems as more of an ad hoc solution[1].

A possible way to extend this work would be to apply perturbation theory. This would mean that the mean-field approach would be left and contributions from more *Slater-determinants* would come into play. Several authors [26][27][28][29][31] have used different sorts of configuration interaction methods but with relatively small basis sets and on small systems. They succeeded in lowering the ground state energy but still have problems with a too large dielectric constant. This is in somewhat of a conflict with the result Reimann et. al.[30] achieved using *local spin density* theory where they succeeded to produce an addition energy spectra that closely resembles Tarucha et. al.s[1] without altering the value of the dielectric constant. It almost seems as if the *spin density* theory somehow includes correlation effects in a better (but in an uncontrolled) way than the configuration interaction calculations yet have done[2]. Maybe the answer lies within perturbation theory.

[1] This opinion might be due to limited knowledge of the nature of the dielectric constant.

[2] This is not entirely true when the configuration interaction calculations have showed the formation of so called Wigner molecules. This is something that the *spin density* calculations fail to do.

Appendix A

B-splines

The theory of B-splines is extensive and therefore it will not be explained in detail here. However to give an intuitive picture of what B-splines really are, the definition and some properties will be explored and the Scrödinger equation for the infinite square well in one dimension will be solved.

A.1 Definition and properties

To construct B-splines one must start with defining a set of points $\{t_i\}$ called the knot set defined on the interval of interest. The only restriction on the knot set is that $t_i \leq t_{i+1}$[1]. The definition of B-splines can be done from the recursion relation below:

$$B_{i,1} = \begin{cases} 1 & \text{if } t_i \leq x < t_{i+1} \\ 0 & \text{otherwise} \end{cases},$$

$$B_{i,k}(x) = \frac{x - t_i}{t_{i+k-1}} B_{i,k-1}(x) + \frac{t_{i+k} - x}{t_{i+k} - t_{i+1}} B_{i+1,k-1}(x), \tag{A.1}$$

where i is the index of a knot point and k is the order of the spline. To differentiate a B-spline the following formulae can be used:

$$\frac{d}{dx} B_{i,k}(x) = (k-1) \frac{B_{i,k-1}(x)}{t_{i+k-1} - t_i} - \frac{B_{i+1,k-1}(x)}{t_{i+k} - t_{i+1}} \tag{A.2}$$

Some properties of B-splines are listed below in a somewhat phenomenological fashion (to get a more mathematical understanding of B-splines see [15]):

- B-splines are piecewise polynomials and are therefore better suited for interpolation than for example pure polynomials.
- If one studies the equation (A.1) one can conclude that at each x only k B-splines are defined. This becomes apparent if one studies figure A.1. But this also implies that in order to define all possible B-splines of order k, the start and end points of the interval of interest must have k knot points.

[1] Note that one can define $t_i = t_{i+1}$.

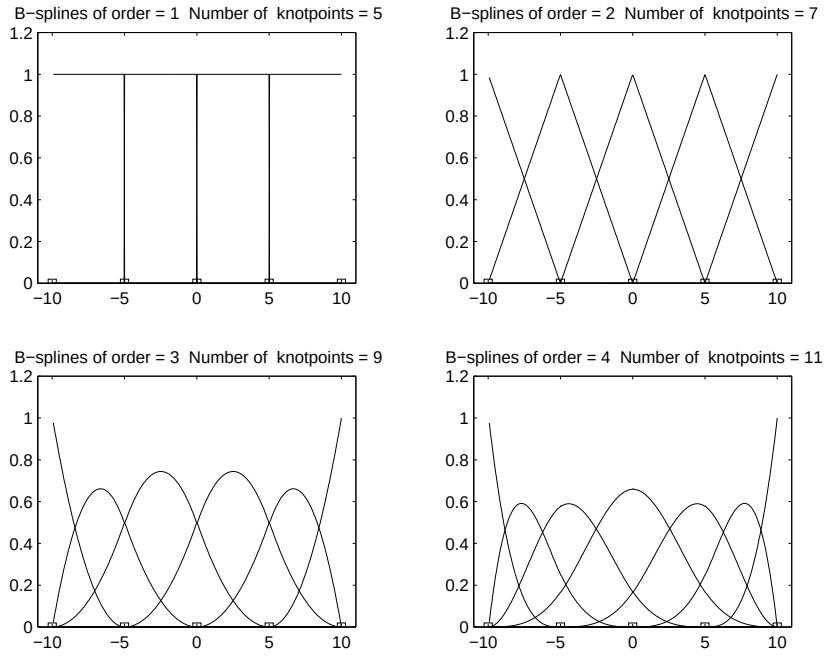

Figure A.1: *B-splines of order* 1 *to* 4 *defined on the interval* $[-10, 10]$. *The start and end points are multiple knot points of order* $k =$ *order of the B-splines. The knot points are marked with* $\square$ *in the plot.*

- A B-spline is non-zero from the i:th knot point to the $(i + k + 1)$:th knot point, that is on k knot point intervals.
- $\sum_i B_{i,k}(x) = 1$. This becomes clear when studying figure A.1.
- $B_{i,k}(x) \geq 0$. This becomes clear when studying figure A.1.
- The $(k - m)$:th derivative is the first discontinuous derivative in a m-fold multiple knot point.
- B-splines form a basis set for the linear space $P_{k,\tau,\nu}$, that is the space of piecewise polynomials of order[2] k with the knot set $\tau = \{\tau_i\}, \tau_i \leq \tau_{i+1}$ with $\nu = \{\nu_i\}$ continuity conditions.

[2]That is, degree$< k$.

A.2 The 1D infinite square well with B-splines

One must start with deciding what interval one wants to calculate things in. Let us choose $[-10, 10]$. This means that the potential becomes

$$V = \begin{cases} 0 & \text{if } -10 \leq x \leq 10 \\ \infty & \text{otherwise} \end{cases}$$

In the chosen interval the Hamilton operator then becomes

$$\hat{H} = -\frac{d^2}{dx^2} \tag{A.3}$$

To make things simple we use a linear knot set. This knot set usually starts and ends with a k-fold knot point where k is the order of the splines. However one must impose the boundary condition that the wavefunctions disappear at the endpoints due to the nature of the potential. This is done by excluding the first and the last B-spline in the set so that the knot set starts and ends with a $(k-1)$-fold knot point. In this way we remove the possibility of having wavefunctions $\neq 0$ at the edges.

The next step is to produce B-splines by equation (A.1) up to the chosen order k.

According to page 10 the Scrödinger equation becomes the following matrix equation:

$$\mathbf{U}^{-1}\mathbf{B}\mathbf{c}_n = E_n\mathbf{c}_n, \tag{A.4}$$

with

$$\mathbf{B}_{ji} = \langle B_j|\hat{H}|B_i\rangle \tag{A.5}$$

$$\mathbf{U}_{ji} = \langle B_j|B_i\rangle \tag{A.6}$$

and

$$|\Psi_n(\mathbf{r})\rangle = \sum_i c_{n,i}|B_i\rangle. \tag{A.7}$$

The $\mathbf{B}_{ij}$ matrix element can be calculated in the following way

$$\mathbf{B}_{ji} = \langle B_j| - \frac{d^2}{dx^2}|B_i\rangle = \langle\frac{dB_j}{dx}|\frac{dB_i}{dx}\rangle \tag{A.8}$$

When performing the integration in (A.5) and (A.6) numerically it is suitable to use Gaussian quadrature because it gives an EXACT result when integrating a polynomial if the right amount of integration points is used.[16]

Then things are straight forward. Solve the eigenvalue problem of equation (A.4), sort the eigenvectors according to the size of the eigenvalues then use equation (A.7) to obtain the wavefunctions. Some results from such calculation are shown in figure A.2.

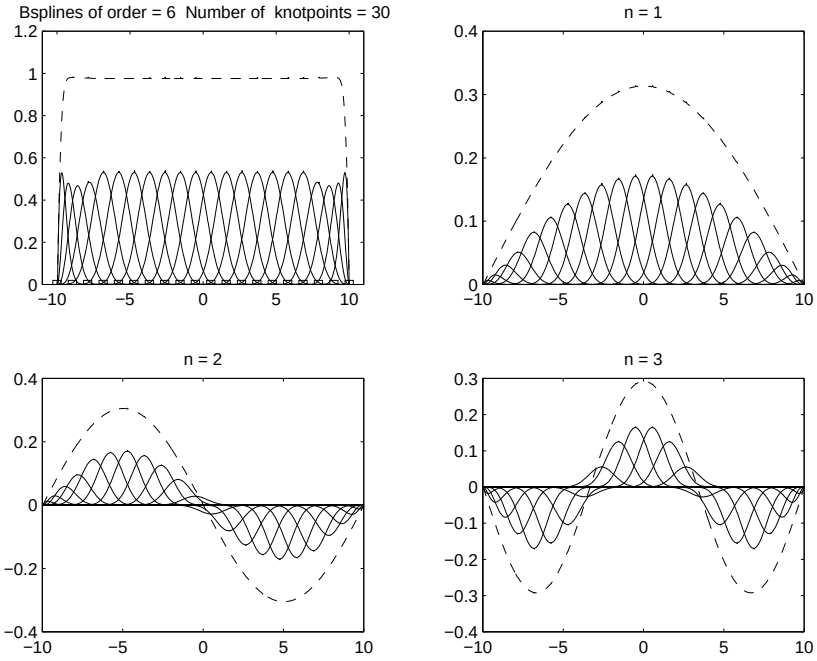

Figure A.2: *The upper left panel shows the B-splines of order $k = 6$ when the first and the last B-spline have been picked out.The B-splines are summed up at each x to give the function $y = 1$. The upper right panel shows the $n = 1$ wavefunction with its B-splines multiplicated with the right coefficients. That is if one adds up the B-splines showing in the plot one obtains the wavefunction. The lower left panel and the lower right panel shows the $n = 2$ and the $n = 3$ wavefunctions respectively in the same way.*

Bibliography

[1] Tarucha, Austing, Honda, van der Hage and Kouwenhoven, 1996, Phys. Rev. Lett. 77, 3613.

[2] Guéret, Blanc, Germann and Rothuizen, 1992, Phys. Rev. Lett. 68, 1896

[3] Ashoori, Stormer, Weiner, Pfeiffer, Baldwin and West, 1993, Phys. Rev. Lett., 71, 613

[4] Meirav, Kastner and Wind, 1990, Phys. Rev. Lett., 65, 771

[5] Kumar, Laux and Stern, 1990, Phys. Rev. B 42, 5166.

[6] Lindgren and Svanberg,1974, ATOMFYSIK .

[7] J.C. Slater, 1950, Phys.Rev,81, 385.

[8] Macucci, Hess, Iafrate, 1993, Phys. Rev. B, 48, 17354.

[9] Macucci, Hess, Iafrate, 1996, Phys. Rev. B, 55, 4879.

[10] Jackson, Classical Electrodynamics third edition,page 111.

[11] Cohl et al., Phys. Rev. A, vol 64, 052509.

[12] N.N. Lebedev, Special Functions and Their Applications (Dover Publications, Inc., 1972)

[13] Segura and Gil, Comput. Phys. Commun. 124(2000)104.

[14] Dreizler and Gross, Density Functional Theory, 1990.

[15] Carl de Boor, A practical guide to splines, 1978.

[16] Peter Pohl, Grunderna i NUMERISKA METODER, 1999.

[17] J.J. Sakurai, Modern Quantum Mechanics Revised Edition, 1994.

[18] Gerald Burns, Solid State Physics, 1990.

[19] J.R Hook & H. E. Hall, Solid State Physics second edition, 1991

[20] Reinmann and Manninen, Rev. Mod. Phys.,74,1283 .

[21] Austing, Tokura, et al., Jpn.J. Appl. Phys.,Part 1, 38, 372.

[22] Koskinen, Manninen and Reimann, Phys. Rev. Lett., vol 79, 1389.

[23] Steffens, Rössler and Suhrke, Europhys.Lett., 42, 529

[24] Mikio Eto, 1997, Jpn. J. Appl. Phys., 36, 3924.

[25] Szafran, Adamowski and Bednarek,2000, Phys. Rev. B, 61, 1971

[26] Yannouelas and Landman, 1999, Phys. Rev. Lett., 82, 5325

[27] Müller and Koonin, 1996, Phys. Rev. B, 54, 14532

[28] Reusch, Häusler and Grabert, 2001, Phys. Rev. B, 63, 113313

[29] Cha and Yang, 2003, Phys. Rev. B, 67, 205312

[30] Reimann, Koskinen, Kolehmainen, Manninen, Austing and Tarucha, 1999, Eur. Phys. J D, 9, 105

[31] Reimann, Koskinen and Manninen, 2000, Phys Rev B, 62, 8108

Acknowledgments

I would like to thank my supervisor, professor Eva Lindroth of the Atomic Physics group at the Department of Physics at Stockholm University. I can not imagen a more helpful supervisor than Eva. Furthermore I appreciate that she has taken all my questions seriously even though they sometimes have been very naive. I would also like to thank my girlfriend, my friends and family for moral support through my ups and downs.